Microstructural evolution during superplastic deformation of Al-Mg-Li alloy: dynamic recrystallization or grain-boundary sliding?

M. Myshlyaev[1,2], G. Korznikova[3], T. Konkova[3,4], E. Korznikova[3], A. Aletdinov[3], G. Khalikova[3,5], G. Raab[6], S. Mironov[7*]

1 Baikov Institute of Metallurgy and Material Science, 49 Lenin-Av., Moscow 119991, Russia
2 Institute of Solid State Physics, 2 Academic Osypian Str., Chernogolovka, Moscow Oblast 142432, Russia
3 Institute for Metals Superplasticity Problems, Russian Academy of Science, 39 Khalturin Str., Ufa 450001, Russia
4 University of Strathclyde, 75 Montrose Str., Glasgow G1 1XJ, United Kingdom
5 Ufa State Petroleum Technological University, 1 Kosmonavtov Str., Ufa 450064, Russia
6 Nosov Magnitogorsk State Technical University, 38, Lenin-Av., Magnitogorsk 455000, Russia
7 Belgorod National Research University, 85 Pobeda Str., Belgorod 308015, Russia

In this work, advanced capabilities of electron backscatter diffraction (EBSD) were applied to evaluate the role played dynamic recrystallization during superplastic deformation of a typical fine-grained material. It was found that the dynamic recrystallization occurred only locally and thus provided only minor contribution to microstructural evolution. Hence, the preservation of the nearly-equiaxed grain morphology, inherent to the superplasticity phenomenon, cannot be attributed to the dynamic recrystallization.

Keywords: Superplasticity; Aluminium alloys; Electron backscatter diffraction (EBSD); Microstructure

1. Introduction

The invention of new technologies in science often enables a new insight into the apparently well-known phenomena. In Materials science, a typical example of such well-established phenomenon is superplasticity. The key microstructural characteristic of this phenomenon is the preservation of nearly-equiaxed grain morphology, despite the colossal plastic strain experienced by the material.Typically, this effect is associated with grain-boundary sliding [e.g. 1-4]. An alternative explanation, however, is the development of dynamic recrystallization [e.g. 5-8], which may provide the rapid subdivision of elongated grains and thus may also maintain the quasi-equiaxed grain shape. Until recently, the limitations of the available experimental techniques did not allow making a final choice between these two theories. The principal difficulties included the experimental observation of grain-boundary sliding as well as the quantification of the extent of dynamic recrystallization. In the recent years, the rapid progress in printing (as well as in analysis) of surface markers has conclusively demonstrated that the grain-boundary sliding, indeed, plays an essential role in superplasticity [e.g. 9]. On the other hand, an application of electron back-scatter diffraction (EBSD) technique has emphasized the importance of the microstructural processes associated with conventional intra-granular slip [e.g. 10-12]. Therefore, although the new technologies have provided a higher level of discussion, the old dilemma “grain-boundary sliding or dynamic recrystallization” is not resolved yet.

This work is part of a research project, which attempts to shed more light on this issue. To this end, EBSD was applied to provide a new insight into the superplasticity phenomenon. In the previous study [11], it was shown that intra-granular slip may play a significant role in superplasticity, at least at comparatively low deformation temperatures. In the present investigation, EBSD was utilized to examine

systematically the microstructural changes occurring during superplastic deformation of a typical fine-grained material over a range of strains (up to 900%). To the best of the authors' knowledge, this is one of the first works in this area. Despite EBSD is not feasible for observation of grain-boundary sliding, this technique is very powerful for detailed characterization of recrystallization. If the extensive development of the latter process would be detected, the present study would be perhaps indicative of the dominant role of dynamic recrystallization in microstructural evolution. Otherwise, it would suggest the key importance of the grain-boundary sliding.

2. Experimental

The material used in the present investigation was a commercial aluminum alloy 1420 (per the Russian designation) with a nominal chemical composition (in wt.%) of Al-5.5Mg-2.2Li-0.12Zr. This is a comparatively simple material whose superplastic behavior is known relatively well. The material was received as a hot-rolled bar with a fully recrystallized microstructure and a mean grain size of 20 μm. To produce a fine-grained microstructure suitable for the superplasticity, the supplied material was solution annealed at 470°C for 1 hour and then subjected to 10 passes of equal-channel angular pressing (ECAP). ECAP was conducted at 370°C (≈0.69T_m, where T_m is the melting point) via route B_C using a die with a 90° square channel[†].
The tension testing specimens for superplasticity tests were machined along the longitudinal axis of the ECAP'ed billet and had a gauge section measuring 12×3×1 mm^3. Based on previous experience, the superplastic tension tests were conducted at 370°C and the nominal strain rate of 3×10^{-2} s^{-1}. The tests were conducted using an Instron 1185 testing machine. To attain thermalequilibrium, the specimens were held at the deformation temperature for 8 min prior the test. To investigate microstructure evolution as function of superplastic strain, the tension tests were interrupted after reaching a series of predetermined degrees of tensile deformation (the further details of this experiment are discussed in Section 3.2).

Table 1. Statistics of EBSD measurements

Material condition	Microstructural region	Scan step size, μm	Size of EBSD map, μm^2	Number of pixels	Number of grains
as-ECAPed	-	0.2	347×243	2,335,983	32,589
as-heated	-		300×300	2,600,367	53,539
30% of tensile deformation	Grip section		300×300	2,600,367	31,692
	Gauge section		350×350	3,537,760	40,593
150% of tensile deformation	Grip section		300×300	2,594,365	39,709
	Gauge section		300×300	2,600,367	19,755
350% of tensile deformation	Grip section		300×280	2,420,306	30,772
	Gauge section		350×350	3,537,761	14,290
500% of tensile deformation	Grip section		300×300	2,600,366	31,246
	Gauge section		400×350	4,043,010	14,474
900% of tensile deformation	Gauge section		393×238	2,703,740	7,024

Note: In all cases, EBSD indexing rate was ≥99.9%.

Microstructural observations were performed mainly by EBSD but selected samples were also additionally studied using transmission electron microscopy (TEM). To ascertain the possible influence of the static storage at deformation temperature, microstructural changes were examined in both the gauge and grip sections of the tension specimens. Moreover, to investigate the microstructure evolved immediately

prior the superplastic tests, a selected sample was water-quenched after the temperature equilibration step. Throughout the manuscript, this sample was referred as the “as-heated” condition. For EBSD measurements, microstructural samples were mounted and then mechanically polished using conventional metallographic techniques; the final surface finish was achieved using 24-hours vibratory polishing with a colloidal silica suspension. EBSD was conducted using a Hitachi S-4300SE field-emission-gun scanning electron microscope equipped with a TSL OIM™ EBSD system and operated at accelerating voltage of 25 kV. The appropriate details of EBSD observations are summarized in Table 1. In order to improve reliability of EBSD data, the grains comprising 3 or fewer pixels were automatically “cleaned” using the standard grain-dilation option of EBSD software. Given the limited angular accuracy of EBSD, boundaries with misorientations below 2° were excluded from consideration. A 15° criterion was applied to differentiate low-angle boundaries (LABs) and high-angle boundaries (HABs). Grain size was quantified using the
equivalent-diameter approach, i.e., assuming each grain as a circle of equivalent area and calculating the associated diameter.
The samples for TEM investigations were obtained by electro-polishing in a 25% solution of nitric acid in methanol at -28°C and a potential of 20 V. TEM observations were performed with a JEM 2100 Plus transmission electron microscope operated at accelerating voltage of 200 kV.

3. Results

3.1. Initial microstructure

The typical microstructure produced during ECAP of the program material is shown in Fig. 1.
It was dominated by the relatively fine (~1 μm) low-aspect ratio grains (Fig. 1a) but also contained some fraction of comparatively-coarse remnants of original microstructure with developed substructure (selected area in Fig. 1a). In terms of size and morphology, the subgrains in such survived fragments were broadly similar to that of the dominant fine-grained microstructure, thus suggesting the prevalence of the continuous recrystallization mechanism‡ during ECAP [e.g. 13]. As a result, grain-size distribution was relatively broad (Fig. 1b), and the produced material contained significant LAB fraction (~30%, Fig. 1c).

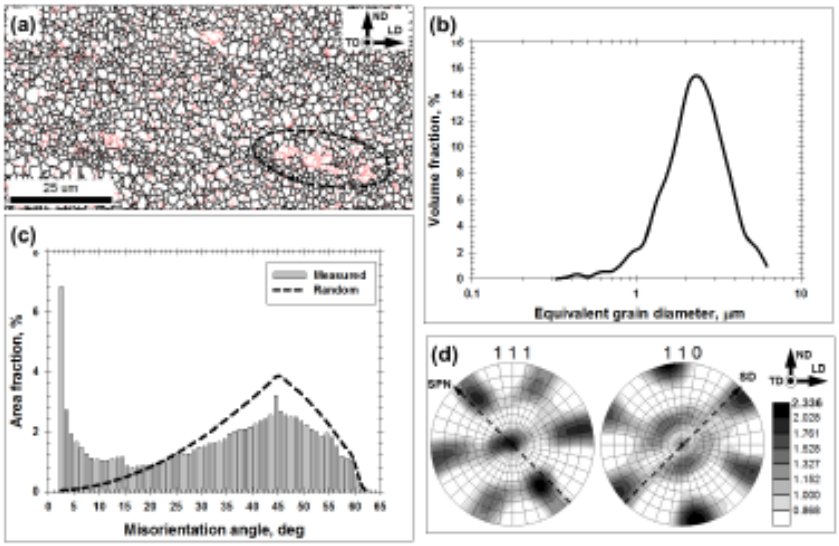

Figure 1. Microstructure of ECAP’ed material: (a) selected portion of EBSD grain-boundary map, (b) grain-size distribution, (c) misorientation-angle distribution, and (d) 111 and 110 pole figures showing

texture. LD, TD, and ND are longitudinal direction, transverse direction, and normal direction of ECAP'ed billet. SPN and SD indicate the presumed orientations of shear plane normal and shear direction during ECAP. In (a), LABs and HABs are depicted as red and black lines, respectively. Note: The selected area in (a) exemplifies continuous recrystallization.

The ECAP'ed material exhibited the simple-shear texture with pronounced $\{hkl\}<110>$ and $B/B\{111\}<112>$ components (Fig. 1d). As expected, the simple-shear texture was rotated relatively the geometry of the produced billet due to the specific orientation of shear plane and shear direction during ECAP (Fig. 1d). Remarkably, the texture was relatively weak (Fig. 1d).
Hence, the misorientation-angle distribution was close to the random distribution associated with a textureless material (Fig. 1c).

3.2. Superplastic behaviour

The typical deformation diagrams recorded during superplastic tests is shown in Fig. 2. Depending on particular experiment, the program material exhibited elongation-to-failure from ≈600% to ≈900%. Moreover, the strain-rate-sensitivity parameter (the *m*-value) was found to be ≈0.4 [11]. Therefore, from a phenomenological standpoint, the material exhibited a typical superplastic behavior.

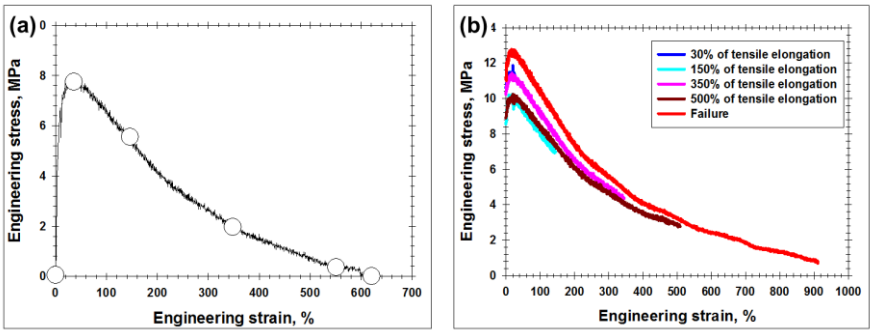

Figure 2. (a) Typical engineering deformation diagram recorded during superplastic test, and (b) a series of engineering diagrams showing the interrupted superplastic tests. In (a), open circles indicate the tensile conditions used for microstructural observations.

The engineering stress-strain diagram showed a typical appearance with a peak and the subsequent decrease of the flow stress (Fig. 2a). In this context, it is worth noting that the tested specimens showed diffused necking after tensile elongation >150% (supplementary Fig. S1). It was likely, therefore, that the observed flow softening was not an intrinsic material-flow characteristic, but was rather attributable to strain localization. It was also clear that the superplastically-deformed material demonstrated the measurable strain hardening at the early stage of material flow.
It is also worth noticing that the superplastically-strained material exhibited pronounced porosity near the failure point (supplementary Fig. S2).

Based on the deformation diagrams, 6 material conditions were selected for investigation of microstructural evolution; those were indicated by open circles in Fig. 2a. To produce these material conditions, a series interrupted tensile tests was conducted, as shown in Fig. 2b.

3.3. Microstructural evolution during superplastic deformation

In order to evaluate the influence of static storage at superplastic temperature, microstructural changes were studied in the *grip* section of the specimens subjected to the interrupted tensile tests. The changes were found to be very small and involved only subtle grain coarsening[§] (supplementary Figs. S3 to S6).

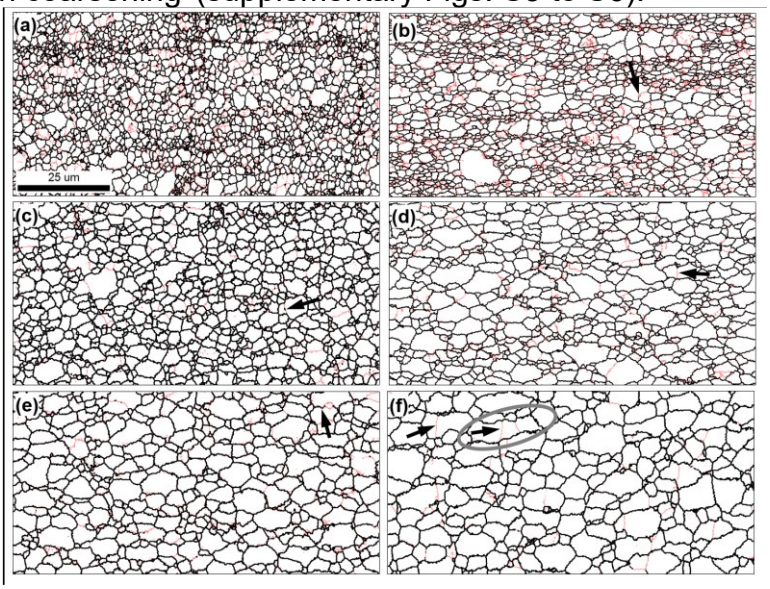

Figure 3. Selected portions of EBSD grain-boundary maps showing microstructure evolution in gauge section of tensioned specimens: (a) the as-heated material condition, and after tensile elongation to (b) 30%, (c) 150%, (d) 350%, (e) 500%, and (f) 900%. In all cases, LABs and HABs are depicted as red and black lines, respectively; tensile direction is horizontal. Arrows exemplify grain fragmentation. Note: The scale bar for all maps is shown in the bottom left corner of (a).

To investigate the effect of superplastic strain, EBSD maps were taken from the *gauge* section of the tensioned specimens. The selected portions of the EBSD maps are shown in Fig. 3 and supplementary Fig. S7. The relevant microstructural statistics derived from EBSD data is summarized in Fig. 4.

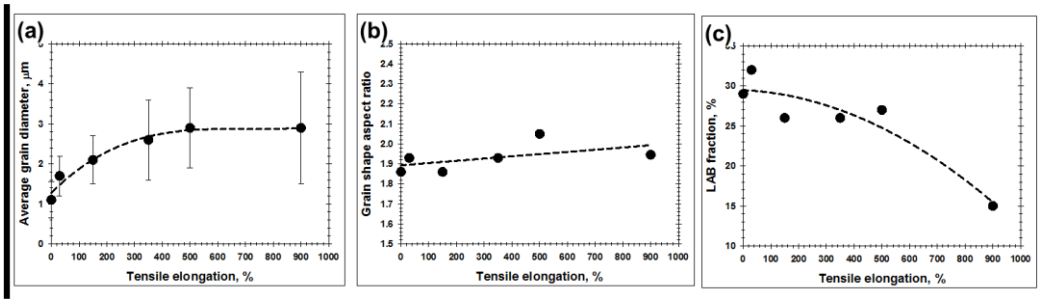

Figure 4. Effect of tensile elongation on (a) mean grain size, (b) mean grain-shape aspect ratio, and (c) LAB fraction in gauge section of tensioned specimens. Error bars in (a) shows standard deviation.

In contrast to the grip section, the superplastically-strained material exhibited the pronounced grain growth (Figs. 3 and 4a). The strain-induced microstructural coarsening is often observed during superplasticity [e.g. 16]. In the present study, the grain growth was most prominent at the early stage of superplastic deformation, but tended to saturate after tensile elongations above ≈350% (Fig. 4a). It is also worth noting that the microstructural coarsening at low strain occurred inhomogeneously, thus resulting in a bimodal grain structure (Figs. 3a and b). After tensile elongation to ≈150%, however, grain size distribution became more or less uniform (Figs. 3c to f). Of particular significance was the observation that the grains maintained the nearly-equiaxed shape throughout the entire studied range of superplastic deformation (Fig.

3). Only negligible increase in the grain-shape aspect ratio was found (Fig. 4b). Despite the superplastically-strained material contained some fraction of elongated grains (an example is circled in Fig. 3f), those represented rather isolated cases and did not reflect the global microstructure evolution.
It is also important to emphasize that superplastic deformation led to a decrease in fraction of LABs (Fig. 4c). From the inspection of EBSD maps in Fig. 3, it is unlikely that this process was attributable to the extensive LAB-to HAB transformation. Hence, it was presumably associated with the observed grain growth.
On the other hand, it should be noted that grains often contained LAB substructure (Fig. 3). Sometimes, the LABs extended across the entire grain interior and even showed a partial transformation to HABs (several examples are arrowed in Fig. 3), thus indicating the grain subdivision process. However, this process was obviously not typical. Therefore, the dynamic continuous recrystallization did not play the dominant role in microstructural evolution.

3.4. Texture development during superplastic deformation

To examine the texture evolution in gauge section of superplastic specimens, orientation data were derived from appropriate EBSD maps and arranged as inverse-pole figures in Fig. 5.

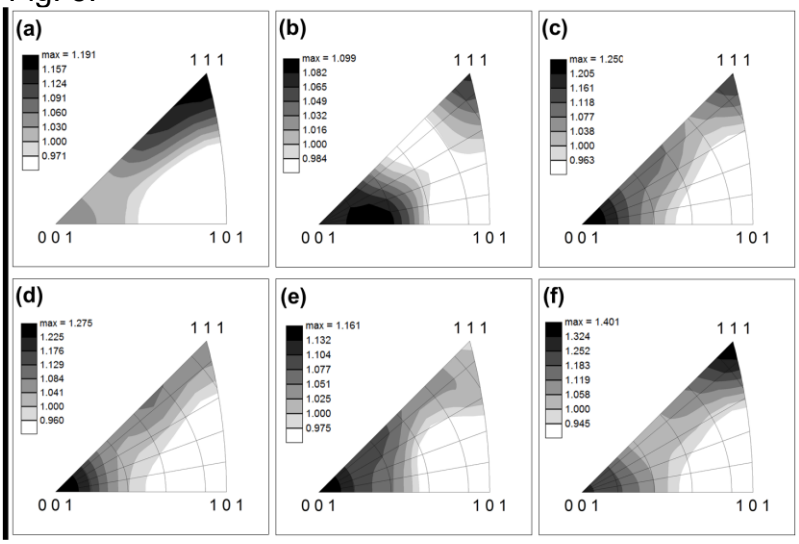

Figure 5. Inverse pole figures showing crystallographic orientation of the material in gauge section of superplastic samples relative tensile direction: (a) immediately before the superplastic test (i.e., after static storage at 370◦C for 8 min), and after subsequent tensile elongation of (b) 30%, (c), 150%, (d) 350%, (e) 500%., and (f) 900%.

In the initial condition, the texture was characterized by an alignment of <111> axes with tensile direction (Fig. 5a). This observation was attributable to the 45-degree rotation of the B / $B\{111\}<112>$ simple-shear texture in ECAP'ed billet (Fig. 1d), as discussed in Section 3.1. Tensile elongation to 30% resulted in shifting of texture peak towards <100> pole (Fig. 5b), thus indicating considerable crystallographic reorientation of grains. The subsequent increase in superplastic strain to 150% and 500% provided the essential orientation spread of <100> peak towards <111> pole, thus giving rise to the specific <100> - <111> texture (Figs. 5c to e). Near the failure point, a substantial strengthening of <111> component was observed (Fig. 5f). In all cases, texture intensity was low.

In aluminum alloys, axial tension usually results in development of either $\{hkl\}<111>$ or $\{hkl\}<100>$ fiber textures [17], which is typically explained in terms of Taylor theory. Specifically, $\{hkl\}<111>$ is usually considered as a stable-end orientation for 8 slip systems, whereas $\{hkl\}<100>$ - for 6 slip systems in face-centered cubic (FCC) crystals. Hence, an increase of the proportion of $\{hkl\}<100>$ component at the expense of $\{hkl\}<111>$ one is typically attributed to a suppression of cross slip. Thus, the observed prevalence of $\{hkl\}<100>$ fiber at superplastic elongations ≤500% (Figs. 5b to e) was likely associated with relatively high Mg content in the program material, which should reduce the stacking fault energy. On the other hand, the observed sharpening of $\{hkl\}<111>$ at very high superplastic strain (Fig. 5f) is less clear. One of the possible explanations for this result may be a diffused necking in the superplastic specimen (supplementary Fig. S1), which should increase local flow stress and thus promote the cross slip.

Anyway, a formation of distinct (through exceptionally weak) tension texture in the present study evidenced a significant role played by the “conventional” intra-granular slip during superplastic deformation. Indeed, TEM observations showed comparatively high dislocation density in some grains (supplementary Fig. S8). In this context, of particular interest is the origin of the transient <100> - <111> component.

It is believed that multiple slip during axial tension of FCC crystals provides crystallographic rotation towards <100> - <111> orientations; for instance, double slip results in the <112> stable end orientation. Hence, the development of the <100> - <111> orientation spread suggests the operation of the comparatively-low number of slip systems within grains. In turn, this may indicate a partial relaxation of strain compatibility requirements at grain boundaries, thus being an indirect evidence of grain-boundary sliding. This concept also explains the extremely low intensity of the measured texture (Fig. 5).

3.5. Orientation correlation between neighboring grains

As shown in Section 3.3, microstructural observations in the present study did not support the concept on the extensive continuous recrystallization during superplastic deformation. On the other hand, the possibility exists that the recrystallization develops very rapidly and therefore this process is difficult to detect experimentally. To evaluate this possibility, the orientation correlation approach [10] was applied in the present study. This technique is based on the idea that continuous recrystallization should result in some orientation correlations between neighboring grains due to the gradual nature of crystallographic rotations of grain fragments away from their common (original) orientation.

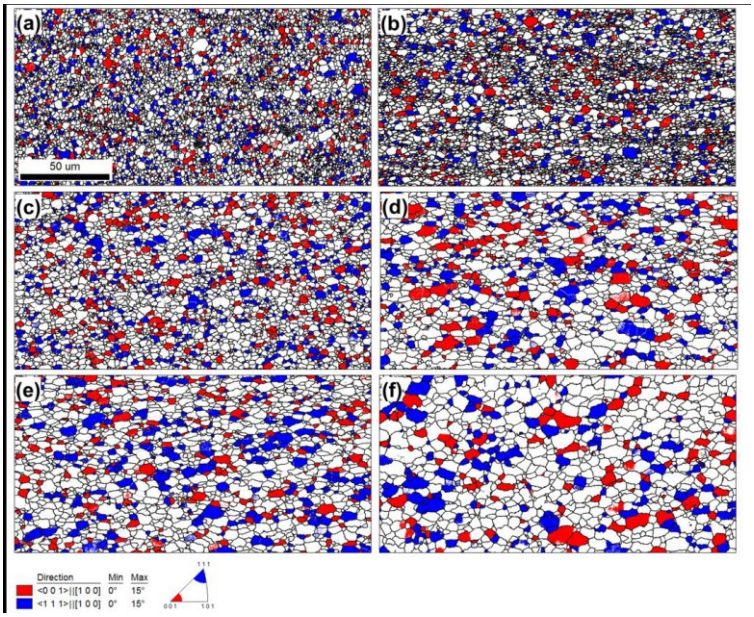

Figure 6. EBSD maps showing spatial distribution of texture components in gauge section of tensioned specimens: (a) in the as-heated material condition, and after tensile elongation to (b) 30%, (c), 150%, (d) 350%, (e) 500%, and (f) 900%. Note: The texture color code is shown in the bottom left corner of the figure. In all cases, HABs are depicted as black lines, while LABs are omitted for simplicity; tensile direction is horizontal. The scale bar for all maps is shown in the bottom left corner of (a).

To examine the possible orientation correlations between the neighboring grains, EBSD texture maps were calculated for different superplastic strains (Fig. 6). In these maps, the spatial distribution of two main texture components, i.e., $\{hkl\}<100>$ (in red) and $\{hkl\}<111>$ (in blue), were shown. It is seen that the components were intermixed with each other in more or less uniform manner, and no clear texture bands were seen. In some cases, however, the grains, which belong to the same texture component, clustered together, thus forming the grain chains aligned with tensile direction. These chains may originate from subdivision of the coarser pre-elongated grains, i.e., from the rapid development of continuous recrystallization.

In this regard, it is interesting to evaluate the possible contribution of this process into global superplastic strain. In a simple model proposed in the previous work [11], it was shown that the relationship between the macro-scale engineering strain e and the grain-shape aspect ratio λ can be expressed as $e \approx (\lambda^{\gamma} - 1) \times 100\%$.

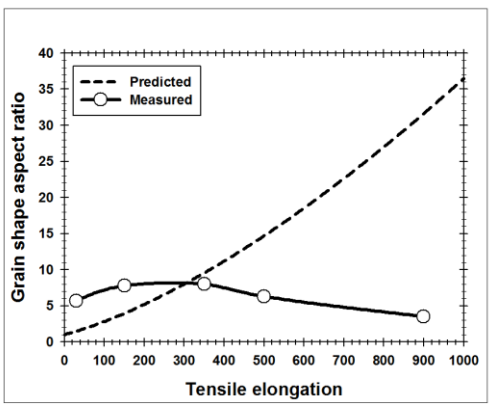

Figure 7. Comparison of the predicted and measured relationships between tensile elongation and the grain-shape-aspect ratio. See Section 3.5 for details

The graphical representation of this equation is given in Fig. 7. From the manual measurements in
EBSD maps in Fig. 6, the *maximal* shape-aspect-ratio of the revealed grain chains was determined for each superplastic deformation and also indicated in Fig. 7. From comparison of the predicted and measurement results, it is seen that microstructure evolution at superplastic strain >350% *cannot* be associated with continuous recrystallization. At lower strain, however, some fraction of grains may evolve via the recrystallization mechanism.

4. Discussion

In the present study, a number of experimental results evidences that superplastic deformation certainly involves an extensive intra-granular slip. Those include the measurable strain hardening (Fig. 2), a development of a typical deformation texture (Figs. 5b to f), as well as the direct TEM observation of an increased dislocation density in grain interior (supplementary Fig. S7).

From the observations, it was also likely that the activity of the intra-granular slip was most pronounced at the early stages of superplastic flow. This finding agreed well with the work by Bate et al. [10]. Furthermore, a noticeable formation of deformation-induced boundaries as well as even the local LAB-to-HAB transformations was also found (Fig. 3b to f, arrows). However, the latter process was obviously not typical for the entire microstructure. This implies a relatively small role played by the continuous recrystallization in the global microstructural evolution.

If so, the nearly-equiaxed grain morphology (Figs. 3 and 4b) cannot be attributed to the rapid development of recrystallization processes. Hence, the simplest explanation for this fact is grain-boundary sliding. This conclusion is consistent with the classical works on superplasticity [e.g., 1-4] as well as with the recent review by Masuda et al. [9]. It is important to point out that superplastic deformation was conducted at the same temperature as the preliminary ECAP (i.e., at 370^{o}C, or ≈0.69T_m). In the case of ECAP, the continuous recrystallization was obviously one of the key microstructural mechanisms, as discussed in Section 3.1. Therefore, it was surmised that the revealed suppression of recrystallization during subsequent superplastic deformation was associated with relatively low strain rate**. The sufficiently slow strain kinetics would allow the spreading of perfect lattice dislocations (associated with the intra-granular slip) into grain-boundary partials and thus may activate grain-boundary sliding. In turn, this should relax the strain compatibility requirements between neighboring grains and thereby reduce the driving force for grain subdivision.

In this context, the most pronounced recrystallization is expected at the early stage of superplastic deformation, i.e., at the relatively high strain rate. The further decrease of the strain rate with superplastic elongation should gradually suppress grain subdivision. This concept agrees with experimental observations.

5. Conclusions

This work was undertaken in order to evaluate the contribution of dynamic recrystallization to microstructural evolution during superplastic deformation of a

typical fine-grained material. To provide thorough insight into microstructural processes, advanced capabilities of EBSD technique were applied. The main conclusions derived from this study are as follows.

(1) A number of experimental observations, including the measurable strain hardening, a formation of typical deformation texture, and an increased dislocation density in grain interiors, evidenced a significant role played by intra-granular slip during superplastic flow.
(2) Nevertheless, dynamic recrystallization was found to occur only locally and thus provided only minor contribution to microstructural evolution. Hence, preservation of nearly-equiaxed grain shape, inherent to the superplastic deformation, cannot be attributed to the dynamic recrystallization.
(3) The suppression of the dynamic recrystallization in superplastic conditions was attributed to the comparatively low strain rate. This should activate grain-boundary sliding and thus relax strain-compatibility requirements for neighboring grains.

Data Availability

The raw/processed data required to reproduce these findings cannot be shared at this time due to technical or time limitations.

Acknowledgements

M. Myshlyaev, S.Mironov, G. Korznikova, A. Aletdinov, G. Khalikova., and T. Konkova gratefully acknowledge financial support from the Russian Fund for Fundamental Research, project No.20-02-00331 A. G. Raab and E. Korznikova were supported under the auspices of a Resolution of the Government of the Russian Federation, April 9, 2010, No. 220, Contract No. 075-15-2019-869. This work was performed using the equipment of the Joint Research Center “Technology and Materials” at Belgorod National Research University (financial support from the Ministry of science and higher education of the Russian Federation under the agreement No. 075-15-2021-690, the unique project identifier RF 2296.61321X0030).

References

[1] M.F Ashby, R.A Verrall, Diffusion-accommodated flow and superplasticity, Acta Metal. 21 (1973) 149-163, https://doi.org/10.1016/0001-6160(73)90057-6
[2] R.C. Gifkins, Superplasticity, creep and grain-boundary sliding, Scripta Metal. 7 (1973) 27-33, https://doi.org/10.1016/0036-9748(73)90174-9
[3] A. Ball, M.M. Hutchinson, Superplasticity in the aluminum-zinc eutectoid, Metal Sci. J., 3 (1969) 1-7; doi:10.1179/msc.1969.3.1.1
[4] T.G. Langdon, A unified approach to grain boundary sliding in creep and superplasticity, Acta Metal. Mater. 42 (1994) 2437-2443, https://doi.org/10.1016/0956-7151(94)90322-0.
[5] R.H. Johnson, C.M. Packer, L. Anderson, O.D. Sherby, Microstructure of superplastic alloys, Phil. Mag. 156 (1968) 1309-1314.
[6] V.A. Likhachev, M.B. Myshlyaev, O.N. Sen’kov, S.P. Belyayev, Creep of aluminum in torsion under superplastic conditions, Phys. Metal. Metallogr. 52 (1981) 156-164.
[7] J.W. Edington, Microstructural aspects of superplasticity, Met. Trans. 13A (1982) 703-715, https://doi.org/10.1007/BF02642384.

[8] A.J. Shakesheff, P.G. Partridge, Superplastic deformation of Al-Li-Cu alloy sheet, J. Mater. Sci. 21 (1986) 1368-1376, https://doi.org/10.1007/BF00553277.
[9] H. Masuda, E. Sato, Diffusional and dislocation accommodation mechanisms in superplastic materials, Acta Mater. 197 (2020) 235-252, https://doi.org/10.1016/j.actamat.2020.07.042
[10] P.S. Bate, N. Ridley, B. Zhang, Mechanical behavior and microstructural evolution in superplastic Al-Li-Mg-Cu-Zr AA8090, Acta Materialia 55 (2007) 4995-5006; https://doi.org/10.1016/j.actamat.2007.05.017
[11] M. Myshlyaev, S. Mironov, G. Korznikova, T. Konkova, E. Korznikova, A. Aletdinov, G. Khalikova, G. Raab, S.L. Semiatin, EBSD study of superplasticity: New insight into a well-known phenomenon, J. All. Compd. 898 (2022) 162949, https://doi.org/10.1016/j.jallcom.2021.162949.
[12] M. Myshlyaev, S. Mironov, G. Korznikova, T. Konkova, E. Korznikova, A. Aletdinov, G. Khalikova, EBSD study of superplastically strained Al-Mg-Li alloy, Mater. Letters 275 (2020) 128063, https://doi.org/10.1016/j.matlet.2020.128063.
[13] F.J. Humphreys, Philip B. Prangnell, Ronald Priestner, Fine-grained alloys by thermomechanical processing,Current Opinion in Solid State and Materials Science 5 (2001) 15-21; https://doi.org/10.1016/S1359-0286(00)00020-6
[14] D.A. Hughes, N. Hansen, High angle boundaries formed by grain subdivision mechanisms, Acta Mater. 45 (1997) 3871-3886; https://doi.org/10.1016/ S1359-6454(97)00027-X.
[15] V.V. Rybin, V.N. Perevezentsev, and Y.V. Svirina, A physical model for the initial stages of the fragmentation of polycrystals in the process of developed plastic deformation, Phys. Metals Metallogr. 118 (2017) 1171-1175; https://doi.org/10.1134/S0031918X17120110
[16] A.K. Ghosh, C.H. Hamilton, Mechanical behavior and hardening characteristics of superplastic Ti-6Al-4V alloy, Metall. Trans. A 10 (1979) 699-706, https://doi.org/10.1007/BF02658391
[17] J. Savoie, Y. Zhou, J.J. Jonas, and S.R. Macewen, Textures induced by tension and deep drawing in aluminum sheets, Acta Mater. 44 (1996) 587-605, https://doi.org/10.1016/1359-6454(95)00214-6
[18] V.M. Segal, Engineering and commercialization of equal channel angular extrusion (ECAE), Mater. Sci. Eng. A 386 (2004) 269-276; https://doi.org/10.1016/j.msea.2004.07.023.
[19] F. Liu, Y. Liu, J. Wang, Estimation of average strain rate during equal-channel angular pressing, Mater. Sci. Forum 850 (2016) 419-425; https://doi.org/10.4028/www.scientific.net/MSF.850.419.